

# Pulse reshaping in photonic crystal waveguides and microcavities with Kerr nonlinearity: Critical issues for all-optical switching

Dragan Vujic\* and Sajeev John

*Department of Physics, University of Toronto, 60 St. George Street, Toronto, Ontario M5S-1A7, Canada*

(Received 30 July 2004; published 11 July 2005)

We delineate critical issues for “controlling light with light” in photonic crystal (PC) waveguides coupled to Kerr-nonlinear microresonators. These arise from (a) fundamental trade-off between switching speed and switching intensity threshold inherent in high-quality  $Q$ -factor cavities and (b) the dynamical nonlinear oscillation of such cavities in response to incident light pulses. Using finite-difference time-domain simulations of electromagnetic pulse propagation, we consider both (i) a nonlinear Fabry-Perot microresonator (embedded within a PC waveguide) exhibiting a narrow transmission resonance and (ii) a nonlinear point defect (side-coupled to a PC waveguide) exhibiting a narrow reflection spectrum. We describe self-induced switching from transmission to reflection induced by pulse intensity tuning as well as control of pulse transmission induced by the secondary, continuous (cw) laser field propagating through the same PC waveguide. For the Fabry-Perot microresonator, a well-defined self-switching threshold is obtained. However, this is accompanied by considerable temporal and spectral distortion of the pulse caused by the oscillatory nonlinear response of the microresonator. When the quality factor of the microresonator is increased, the switching intensity threshold can be lowered but the pulse transit (switching) time and the pulse distortion are increased. For the side-coupled microresonator, a gradual (not sharp) self-switching behavior as a function of incident intensity is obtained. For both the Fabry-Perot and side-coupled nonlinear microresonators, control of pulse transmission can be achieved by means of a secondary cw laser field. The cw power required for switching with realistic Kerr nonlinearities is in excess of  $1 \text{ W}/\mu\text{m}^2$  and may cause optical damage to the semiconducting PC backbone. Both instantaneous and noninstantaneous Kerr-response models are considered. Our results underscore the limitations and trade-offs inherent in the possible control of light with light using Kerr-nonlinear microresonators.

DOI: [10.1103/PhysRevA.72.013807](https://doi.org/10.1103/PhysRevA.72.013807)

PACS number(s): 42.65.Pc, 42.70.Qs

## I. INTRODUCTION

Photonic band-gap (PBG) materials [1,2] are periodic dielectric structures capable of guiding light through subwavelength-scale circuit paths using the mechanism of light localization [3]. This occurs through multiple light scattering and interference rather than total internal reflection or “refractive-index guiding.” A specific embodiment of the diffractionless flow of light in an optical microchip has been demonstrated in two- and three-dimensional (2D-3D) PBG heterostructures [4]. These photonic crystals (PC’s) may be viewed as the optical analog of semiconductors and may facilitate micromanipulation of laser light in the same way that semiconductors control electric currents [5–7]. This makes them attractive for integrated optics and applications in telecommunications. One important ingredient in this application is the possibility of all-optical switching—i.e., devices that alter the propagation of one laser beam if the intensity of a second laser beam changes slightly. This requires the use of nonlinear photonic crystals in which the refractive index is controllably altered by the incident light intensity in specific regions. One recently proposed mechanism for “controlling light with light” involves the engineering of the electromagnetic vacuum density of states in a three-dimensional PBG microchip [8–10]. Here, a multimode waveguide chan-

nel is engineered such that one or more of the waveguide modes exhibits a sharp frequency cutoff. This leads to a very large (factor of 100 or more) and sudden (over a range of  $10^{-4}$  of the optical frequency) change in the local electromagnetic density of states (LDOS) at specific frequencies [11]. If quantum dots are placed near the waveguide channel with resonant optical transition near this LDOS discontinuity, the resonant nonlinear optical response of the active regions exhibits sudden switching from absorptive to amplifying (negative absorption coefficient) behavior as the optical pumping intensity is increased [10,11]. A small modulation ( $\sim 5 \text{ nW}$ ) in the pump field can thereby facilitate coherent switching of the propagation characteristics of a second laser beam passing through the same waveguide channel.

A more traditional mechanism for controlling light with light is based on nonresonant Kerr nonlinearity and high-quality ( $Q$ ) factor optical cavity resonances. The simplest version of this mechanism consists of a Fabry-Perot resonator filled with weakly nonlinear (nonresonant)  $\chi^{(3)}$  medium. By pumping the nonlinear medium with an intense laser field, it is possible to shift the transmission resonance of the Fabry-Perot cavity, thereby switching the transmission characteristics of a second probe beam that is tuned to Fabry-Perot resonance frequency [12]. This concept can also be applied, in a miniaturized embodiment, using photonic crystal microcavities coupled to suitable single-mode waveguides. It has been shown theoretically that optical bistability can be achieved [13–16] in photonic crystal

\*Electronic address: [dvujic@physics.utoronto.ca](mailto:dvujic@physics.utoronto.ca)

waveguides coupled to a high- $Q$  microcavity, with a non-resonant Kerr nonlinearity. Unlike all-optical switching based on electromagnetic vacuum (density of states) engineering in a multimode PBG waveguide [9,8,17], the microcavity (with nonresonant Kerr nonlinearity) couples directly to the waveguide and locally alters the group velocity of light in the waveguide at frequencies near the cavity resonance.

In this paper we delineate the fundamental trade-off in the functionality of photonic crystal optical switching devices based on microcavity resonators and Kerr nonlinearity. This trade-off is a direct consequence of the conjugate relation between spectral width and temporal duration of wave phenomena. The spectral width of the cavity resonance determines the intensity of light required to nonlinearly shift the cavity in and out of resonance with central frequency of an incident pulse. The temporal duration required for the incident pulse to be transmitted through the cavity as well as the time scale of response of the cavity resonance to the optical field determines the optical switching time. The inverse relation between optical switching intensity threshold and the switching time scale has been a limiting factor, critical to the development of optical transistor action in nonlinear Fabry-Perot étalons [12]. In a photonic crystal, on the other hand, there is considerably greater focusing of electromagnetic field intensity within subwavelength-scale waveguide apertures [13–16], leading to lower overall power requirements than in conventional Fabry-Perot architectures [12]. It nevertheless remains a fundamental challenge to achieve subpicosecond switching with microwatt level power in any nonlinear cavity-based architecture. In order to optically shift the cavity transmission resonance with low intensity light, a narrow high- $Q$ -factor resonance is required. However, a narrow resonance implies that the cavity buildup time (required for a pulse to enter and leave the cavity) is prolonged, leading to slower optical switching.

In order to highlight the universal nature of the critical issues, we provide, from the outset, a semiempirical scaling relation that summarizes the trade-off between switching time and switching intensity threshold for the three illustrations presented later in our paper. In addition to providing a physical picture, this allows readers to extrapolate our results to different nonlinear materials than we illustrate. We begin with the fundamental conjugacy relation between the cavity spectral width,  $\Delta\omega^T$  (full width at half maximum for the transmission spectrum of the cavity) and cavity buildup time  $T_{cavity}$ . For the Lorentzian spectrum, this takes the form

$$\left(\frac{\Delta\omega^T}{2}\right)(T_{cavity}) = 1. \quad (1)$$

The cavity spectral width is related to the cavity quality factor  $Q$  by the relation  $\Delta\omega^T = \omega_{res}/Q$  where  $\omega_{res}$  is the central frequency of the cavity resonance for small light intensities. In order to reduce the low-intensity transmission below 10%, one must detune the pulse central frequency  $\omega_0$  from  $\omega_{res}$  by at least  $3\Delta\omega^T/2$ . For short pulses it should be much larger because of the strong overlap of the part of the pulse spectrum and cavity transmission spectrum.

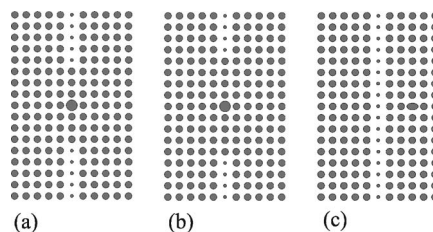


FIG. 1. Three types of defect cavities: (a) Low- $Q$ -factor Fabry-Perot resonator in photonic crystal (PC) waveguide. (b) High- $Q$ -factor Fabry-Perot resonator in PC waveguide. These two types of cavities are engineered by adding one high-dielectric rod with radius  $5a/12$  ( $a$  is the lattice constant) and three or four standard high-dielectric rods of radius  $a/4$  on both sides in the defect line. (c) Side-coupled microcavity (shown as elliptical rod with long axes of  $a/2$  and short axes of  $a/4$ ). All rods are assumed to exhibit a nonlinear Kerr coefficient (see text)  $n_2 = 1.5 \times 10^{-17} \text{ m}^2/\text{W}$  and linear refractive index  $n_H = 3.5$ . The background dielectric (white region) is assumed to be linear with a refractive index of  $n_L = 1.5$ .

From numerical analysis, we find a simple scaling rule for all three cavity architectures we study in this paper (Fig. 1). In particular, a displacement in frequency of the cavity resonance requires a shift in the dielectric constant of the defect rod by an amount

$$\frac{|\Delta\epsilon|}{\epsilon_{res}} \approx n_0 |\Delta\omega_{shift}| / \omega_{res}, \quad (2)$$

where  $\epsilon_{res}$  is the linear dielectric constant of the defect rod and  $n_0 = \sqrt{\epsilon_{res}}$  is the corresponding refractive index. For a system with noninstantaneous (see Sec. II) Kerr coefficient  $n_2$ , this shift in dielectric constant requires a field (time-averaged) intensity  $I$  satisfying the relation

$$\Delta\epsilon = 2n_0 n_2 I, \quad (3)$$

where  $n_0$  is the weak-field refractive index and  $n_2$  is the Kerr coefficient.

Finally the overall switching time scale of the device,  $T_{switch}$ , defined by the sum of (i) time interval needed for the light beam to switch the optical gate from the position off/on to position on/off and (ii) the time taken by the pulse to cross a cavity.  $T_{switch}$  is, usually, a few times larger than  $T_{cavity}$ . In any event  $T_{switch} \geq T_{cavity}$ . This leads to a scaling relation of the form

$$\left|\frac{\Delta n}{n}\right| \geq \frac{3n}{2T_{cavity}\omega_{res}}. \quad (4)$$

According to this simple analysis, we find that for subpicosecond switching of a pulse with  $1.55 \mu\text{m}$  vacuum wavelength, we have to provide a  $Q$  factor of less than 600 and a relative index change of defect rod of almost a half of a percent. Since the nonlinear effect does not change the dielectric constant uniformly, in practice the peak index change is even higher. This extremely high value is not suited to conventional Kerr materials.

Further critical issues for all-optical switching devices, based on microcavities in PC's made of Kerr-type nonlinear materials, arise from distortion of transmitted information. In

order to reduce pulse shape distortion during the interaction and transmission process through the cavity region, it is necessary to use pulses with duration much longer than the cavity buildup and decay time. When a slightly off-resonance pulse enters the microcavity resonator, the resonance frequency of the cavity is shifted toward the pulse center frequency. This allows more of the pulse to enter, leading to an overshoot in the cavity resonance beyond the pulse center frequency. This in turn allows less of the pulse to enter the cavity and the cavity resonance reverts to its original position. This process can repeat itself, leading to oscillations in the cavity refractive index, the cavity resonance central frequency, and the transmission spectrum of the switching device. As a result the pulse spectral features and temporal profile can be severely distorted. Moreover, the nonlinear effect changes the  $Q$  factor of the cavity itself in an oscillatory manner. These phenomena are universally observed when dealing with high- $Q$  (greater than 1000) cavities and short (picosecond-scale) pulses. The details of these phenomena are different for different architectures. Accordingly, we provide detailed numerical illustrations of these effects in these distinct photonic crystal microresonators. We evaluate the optical power level and switching time scales in single-pulse propagation. We determine the transmitted pulse energies as well as details of the pulse reshaping, distortion, and delay as an incident pulse interacts with the nonlinear microresonator. We demonstrate that in addition to the trade-off between switching intensity threshold and switching time, higher  $Q$  factors lead to increased temporal distortion of the pulse profile due to oscillations in the nonlinear dielectric constant of the microcavity. Finally, we consider the combined effects of a steady-state laser beam (holding field) and fast optical pulse passing through the PC waveguide coupled to the nonlinear microcavity. For very intense holding fields, it is possible to amplify the pulse by transfer of energy from the holding field through the nonlinear microcavity.

Unlike earlier studies [13–16], we use the noninstantaneous as well as instantaneous Kerr model of nonlinearity and we consider the switching process in greater detail. Switching of the pulse is not only a consequence of changing the band structure with the signal beam or control beam, but through active interaction and feedback between the microcavity properties and the respective beams.

Section II of the paper defines structures for investigation and introduces basic equations. Section III contains an analysis of the pulse propagation through three different structures. Section IV discusses the influence of a continuous wave (holding field) on pulse propagation, and Sec. V summarizes our overall conclusions.

## II. MODEL

We study optical switching in an idealized two-dimensional photonic crystal composed of rods of high-index material embedded in a low-index material. This idealized 2D system (with no propagation allowed normal to the 2D plane) is expected to mimic the behavior of a more realistic 2D-3D PBG heterostructure [4] in which 2D confinement of light occurs through a planer PC microchip layer that is suit-

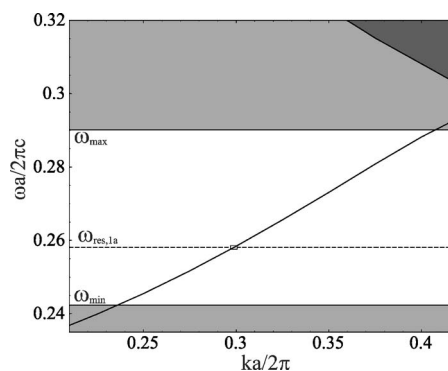


FIG. 2. Dispersion relation for the photonic crystal waveguide, shown in Fig. 1, as a function of wave vector  $k$  along the waveguide axis. The dashed line shows the resonant frequency  $\omega_{res,1a}$  of the low- $Q$ -factor Fabry-Perot resonator of Fig. 1(a). The small rectangle approximately borders the frequency spectrum which can cross the cavity. The 2D photonic band gap is bounded by frequencies  $\omega_{min}$  and  $\omega_{max}$ .

ably embedded in a 3D PBG material. The idealized 2D structure consists of a square-lattice photonic crystal (lattice constant  $a$ ) of high-dielectric rods ( $n_H=3.5$ ) with radius of  $a/4$ , embedded in low-dielectric material ( $n_L=1.5$ ). This idealization describes a periodic array of parallel rods whose axial length (and aspect ratio) is infinite and for which we consider only electromagnetic propagation vectors that are normal to the rod axes. In a typical photonic crystal membrane [18,19] or PBG-heterostructure-based microchip layer [4] the actual vertical thickness of the chip is less than  $1 \mu\text{m}$ , for circuits operating at  $1.5 \mu\text{m}$  wavelength. For our 2D model, we describe electromagnetic power in a waveguide channel in units of watts per unit length normal to the 2D microchip plane. The idealized 2D structure has a band gap for transverse-magnetic (TM) polarized light, between  $\omega_{min}=0.24(2\pi c/a)$  and  $\omega_{max}=0.29(2\pi c/a)$ . A single-mode waveguide (Fig. 2) is constructed by reducing the radius of rods in one line to  $a/12$ . We consider two different types of defect cavities. The first type of a resonant cavity is engineered by adding one rod with larger radius of  $5a/12$  and three [Fig. 1(a)] or four [Fig. 1(b)] rods with standard radius on both sides of the large one within the waveguide channel. This type of architecture leads to a narrow frequency band of transmission through the waveguide near the microcavity resonance. The second type of cavity is created by introducing a point defect with an elliptical dielectric rod, with long axis of  $a/2$  and short axis of  $a/4$  adjacent to the waveguide channel [see Fig. 1(c)]. This type of architecture leads to a narrow frequency band of reflection in the waveguide near the defect resonance. Numerical, finite-difference time-domain (FDTD) simulations of light propagation along the waveguide [for the structures given in Figs. 1(a) and 1(c)] are performed at a resolution of 12 pixels per lattice constant  $a$ , while linear and nonlinear optical propagation characteristics of the structure shown in Fig. 1(b) are calculated with resolution of 24 pixels per lattice constant.

The first two cavities have Lorentzian transmission spectrum allowing 100% of transmission only for frequency equal to the resonant frequency of defect cavities which are

$\omega_{res,1a}=0.2581(2\pi c/a)$  and  $\omega_{res,1b}=0.2612(2\pi c/a)$ . The cavity shown in Fig. 1(c) gives a “notch filter” response in the transmission spectrum around the resonant frequency  $\omega_{res,1c}=0.2646(2\pi c/a)$ . In order to determine the quality factors  $Q$  of the resonant cavities we introduce a weak source excitation where the  $z$  component of the electric field takes the form of a Gaussian pulse in time:

$$E_z(t) = e^{[(t-3\tau_p)/\tau_p]^2} \sin(t-3\tau_p), \quad (5)$$

where the parameter  $\tau_p$  is chosen to cover the frequency range of interest. Here we consider only the linear optical response of the material. When the pulse impinges on the defect, there is a buildup of energy in the cavity, after which the energy decays back into the waveguide. During this final decay, the amplitude of the field in the defect decreases exponentially:

$$A(t) = A(0)\exp\left(-\frac{t}{\tau}\right). \quad (6)$$

The quality factor is defined by the relation  $Q = \omega_{res}\tau/2$  and we obtain the values  $Q_{1a}=538$ ,  $Q_{1b}=2483$ , and  $Q_{1c}=1055$ .

We investigate the light propagation in nonlinear photonic crystals with waveguide and microcavity using the FDTD method [20,21]. We assume nonresonant third-order ( $\chi^{(3)}$ ) optical nonlinearity in the high-index material only, while the low-index material is linear. The refractive index of many materials can be described by the relation [22]  $n = n_0 + \Delta n = n_0 + n_0 c \epsilon_0 n_2 \langle E^2 \rangle$ , where  $n_0$  is the weak-field refractive index,  $c$  is the speed of light in vacuum,  $\epsilon_0$  is the permittivity of free space, and  $n_2$  is the Kerr coefficient. Here the response of the medium is noninstantaneous and the angular brackets represent a time average of the electric field intensity, over an optical cycle. We refer to this as the “noninstantaneous model.” For purely comparative purposes, we concurrently study the “instantaneous model”  $n = n_0 + n_0 c \epsilon_0 n_2 E^2$ . This model was used in previously published literature [13]. In general, the noninstantaneous model is a more realistic description of picosecond pulse propagation in typical semiconductors. Materials with much faster response (on the time scale of a single optical period) typically have very weak nonlinearity. The noninstantaneous model requires modification in the context of femtosecond-scale pulses [23]. However, in the context of high- $Q$ -factor microcavities, femtosecond pulses will be severely stretched due to cavity buildup and decay times. We restrict ourselves to pulses of sufficient duration such that the noninstantaneous model is physically the more relevant one and we consider the noninstantaneous model for mathematical comparison only.

Restricting ourselves to the TM polarization, Maxwell’s equations in 2D reduce to

$$\frac{\partial D_z}{\partial t} = \left( \frac{\partial H_y}{\partial x} - \frac{\partial H_x}{\partial y} \right), \quad (7)$$

$$\mu_0 \frac{\partial H_x}{\partial t} = -\frac{\partial E_z}{\partial y}, \quad (8)$$

$$\mu_0 \frac{\partial H_y}{\partial t} = \frac{\partial E_z}{\partial x}, \quad (9)$$

where  $(H_x, H_y)$  are components of the magnetic field,  $E_z$  is the electric field, and  $\mu_0$  is the permeability of free space. The electric displacement  $D_z$  is given by the equation

$$D_z = \epsilon_0 n^2 E_z \approx \epsilon_0 (n_0^2 + 2n_0 \Delta n) E_z. \quad (10)$$

Maxwell’s equations (7)–(9) can be simplified by introducing the approximate relation

$$\frac{\partial D_z}{\partial t} = \epsilon_{nl} \frac{\partial E_z}{\partial t}, \quad (11)$$

involving the nonlinear dielectric function  $\epsilon_{nl}$ .

For the noninstantaneous model we use the approximate form

$$\epsilon_{nl} = \epsilon_0 n_0^2 [1 + c \epsilon_0 n_2 |A(x, y, t)|^2], \quad (12)$$

where  $A$  is the slowly varying envelope of the electric field, satisfying the relation  $\langle E_z^2 \rangle = \frac{1}{2} A^2$ . Here we assume that the time dependence of  $\epsilon_{nl}$  is slow compared to the optical period, so in the noninstantaneous model, we simply took intensity out of the differentiation.

For the instantaneous model we include the full time dependence of the nonlinear dielectric and obtain

$$\epsilon_{nl} = \epsilon_0 n_0^2 [1 + 6c \epsilon_0 n_2 |E_z(x, y, t)|^2]. \quad (13)$$

For illustration, we choose the Kerr coefficient in the high-index rods to be  $n_2 = 1.5 \times 10^{-17} \text{ m}^2/\text{W}$ , corresponding to AlGaAs [24]. The background dielectric is assumed to be linear ( $n_2=0$ ).

We studied influence of a continuous wave on pulse propagation through the waveguide by providing two independent inputs, one in the form of pulse, Gaussian in time, with central frequency  $\omega_0$ , and one in the form of a continuous wave oscillating at different frequency  $\omega_{cw}$ , where  $|\omega_{cw} - \omega_0|$  is much larger than the bandwidth of the pulse. In that case Maxwell’s equations can be separated into two coupled sets of equations, one to describe pulse propagation and one for continuous wave. These two sets of equations are connected only through nonlinear effect, Eqs. (12) and (13), where we have to use the full electric field which is a superposition of both  $E_z(x, y, t) = E_z^p(x, y, t) + E_z^{cw}(x, y, t)$ . Supercripts  $p$  and  $cw$  stand for pulse and continuous wave, respectively.

### III. PULSE PROPAGATION

In order to study the nonlinear switching behavior, we launch pulses whose envelope is Gaussian in time, with full width at half maximum (FWHM)  $\Delta\omega = 0.00022(2\pi c/a)$  into the input waveguide. As a result of the interaction with the defect cavity, the waveguide is transferred to one mini-waveguide (Fig. 2) allowing propagation of a very narrow frequency spectrum around the resonant frequency. The power transmission spectrum has Lorentzian shape with full width at half maximum  $\sim 0.0005(2\pi c/a)$ . Our aim is to see

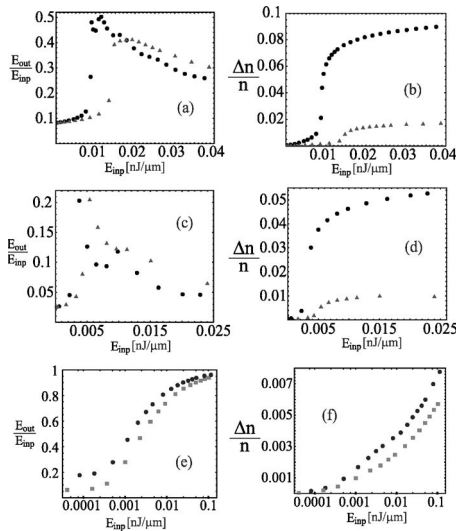


FIG. 3. (a) Transmission energy  $E_{out}$  relative to pulse input energy  $E_{inp}$  of the pulse propagating through the waveguide shown in Fig. 1(a) as a function of input pulse energy for the instantaneous (black circles) and noninstantaneous (grey triangles) models. The pulse envelop is Gaussian in time with full width at half maximum  $\Delta\omega=0.00022(2\pi c/a)$ , detuned from the linear resonance by  $\omega_{res}-\omega_0=0.0008(2\pi c/a)$ . (b) Maximal index change  $\Delta n/n$  induced by the pulse from part (a). (c) Transmission energy and (d) maximal induced index change for the pulse propagating through the structure depicted in Fig. 1(b), for the instantaneous (black circles) and noninstantaneous (grey triangles) models. The pulse is detuned from the linear resonant frequency for the amount of  $0.00035(2\pi c/a)$ . The pulse shape and width are the same as in part (a). (e) and (f) describe the pulse transmission and relative index change for a pulse propagating through the waveguide depicted in Fig. 1(c). The central frequency of the pulse is equal to the resonant frequency of the cavity and the pulse shape and width are the same as in part (a) (black circles), while grey squares refer to a pulse with twice longer duration [ $\Delta\omega=0.00011(2\pi c/a)$ ]. Only the noninstantaneous model is considered. In all cases, the Kerr coefficient (see text) is  $n_2=1.5\times 10^{-17}$  m<sup>2</sup>/W.

if the nonlinear effect can be used as a gate for pulse propagation through this waveguide. As the first numerical experiment we study the properties of pulses with central frequency  $\omega_0=0.2573(2\pi c/a)$  propagating through the nonlinear photonic crystal given on Fig. 1(a). Similarly to earlier studies [13], we find that for low enough light intensity the transmission is small because the pulse is off resonance. However, sufficiently high light intensity can locally change the band structure and the cavity resonance frequency in order to allow switching from pulse reflection to transmission. Comparing the results of the instantaneous and noninstantaneous Kerr nonlinearities, we find that the switching threshold in the instantaneous model occurs for lower light intensities than in the noninstantaneous model. The transmitted energy through the microcavity resonator on threshold is about 49% in the instantaneous model, whereas it is about 40% in the noninstantaneous model [see Fig. 3(a)]. A more significant difference between these two models is the peak nonlinearity induced by the pulse. We find that the maximal relative change of the refraction index in the noninstanta-

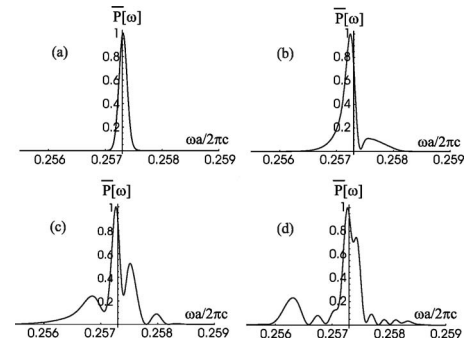


FIG. 4. (a) Normalized output power of the pulse propagating through the waveguide shown in Fig. 1(a) using the instantaneous model (see text) of nonlinear Kerr response: (a) for the pulse energy slightly below the threshold ( $E_{inp}=5.3$  pJ/ $\mu$ m), (b) on the threshold ( $E_{inp}=9$  pJ/ $\mu$ m), (c) for the pulse having highest transmission ( $E_{inp}=11$  pJ/ $\mu$ m), and (d) for the pulse much above the threshold ( $E_{inp}=28$  pJ/ $\mu$ m). Here, the input pulse envelop is a Gaussian in time with full width at half maximum  $\Delta\omega=0.00022(2\pi c/a)$  and the Kerr coefficient is the same as in Fig. 3.

neous model is smaller than 1% at threshold. This value is a few times smaller than in the instantaneous model. Nevertheless, for both models, the refractive index change required for switching is much much higher than the typical values used in optoelectronic devices in this frequency range [25]. While a smaller refractive index modulation could be used in the context of the higher- $Q$ -factor cavity, this would lead to the slower switching due to the cavity buildup and relaxation time.

One of the most important questions concerning optical switching is whether the information carried by the pulse is retained after crossing the cavity. In order to answer this question, we plot the pulse spectral distribution of the transmitted power for both models in Figs. 4 and 5. There is a large dispersion of the spectrum above the threshold, corresponding to significant temporal pulse distortion. This is a

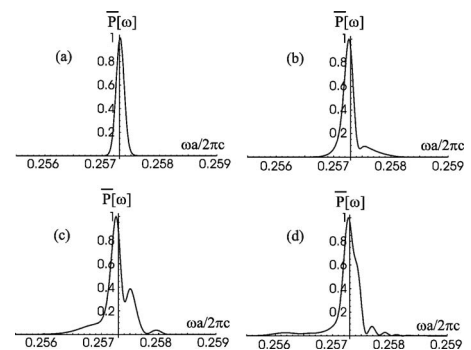


FIG. 5. (a) Normalized output power of the pulse propagating through the waveguide shown in Fig. 1(a) using the noninstantaneous model (see text) of nonlinear Kerr response: (a) for the pulse energy slightly below the threshold ( $E_{inp}=8.5$  pJ/ $\mu$ m), (b) on the threshold ( $E_{inp}=16$  pJ/ $\mu$ m), (c) for the pulse having highest transmission ( $E_{inp}=19$  pJ/ $\mu$ m), and (d) for the pulse much above the threshold ( $E_{inp}=34$  pJ/ $\mu$ m). Here, the input pulse envelop is a Gaussian in time with full width at half maximum  $\Delta\omega=0.00022(2\pi c/a)$  and the Kerr coefficient is the same as in Fig. 3.

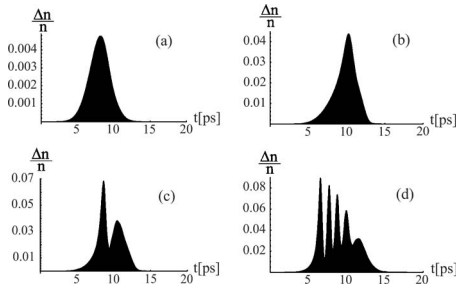


FIG. 6. Time dependence of refractive index change  $\Delta n/n$  for the instantaneous model of nonlinear Kerr response, measured at one point, in the large defect rod, near its front surface and in the middle of the defect line, (a) for the pulse below the threshold ( $E_{inp}=5.3 \text{ pJ}/\mu\text{m}$ ), (b) on the threshold ( $E_{inp}=9 \text{ pJ}/\mu\text{m}$ ), (c) for the pulse with highest transmission ( $E_{inp}=11 \text{ pJ}/\mu\text{m}$ ), and (d) much above the threshold ( $E_{inp}=37 \text{ pJ}/\mu\text{m}$ ). The other characteristics of the input pulse are described in the caption of Fig. 3(a).

major hindrance for applications in optical telecommunications. This pulse dispersion is a consequence of the temporal and spatial profile of the nonlinear index change in the defect cavity. In Fig. 6 we present the temporal behavior of the relative index change at one point near the front surface of the large rod shown on Fig. 1(a). When the pulse arrives at the cavity, a large part of the pulse energy is reflected because the pulse is off resonance. Only a small part of the pulse energy, oscillating near the linear resonance, can reach the cavity. As a result of nonlinearity, the incident light changes the properties of the cavity (resonant frequency), allowing a more significant part of the pulse energy to reach the cavity. The biggest part of the input pulse energy can reach the cavity when the new resonant frequency reaches the value  $\omega_0$ . But the light intensity continues to increase, because of cavity buildup time as well as because of the increase of the amplitude of the incoming field. Accordingly, the new instantaneous resonant frequency overshoots the target value of  $\omega_0$  and access to the input light can be prohibited again. If the input light intensity is high enough, the instantaneous resonant frequency (induced by nonlinearity) will exhibit oscillations. This ringing behavior in the nonlinear cavity contributes to significant dispersion in the transmitted spectrum and distortion of the pulse temporal profile. The period of oscillation depends on the cavity buildup time and input light intensity. If the input intensity is near the threshold, the instantaneous resonant frequency will reach the value  $\omega_0$ , close to the time when the input amplitude is the highest, allowing a large transmission of pulse energy. If the input pulse intensity is even higher, oscillation of the induced resonant shift is established around a value smaller than  $\omega_0$ , leading to a decrease of transmission.

Similar numerical experiments were repeated with a structure containing a cavity with higher  $Q$  factor [Fig. 1(b)]. However, in this case the pulse central frequency was tuned closer to the linear cavity resonance [ $\omega_{res}-\omega_0=0.00035(2\pi c/a)$ ] for good switching. We found qualitatively similar behavior as for the structure 1(a). However, the transmission for the higher- $Q$  cavity is about half that of the lower- $Q$  cavity at the threshold [Fig. 3(c)]. Working with cavities with a higher  $Q$  factor has advantages and disadvan-

tages. A smaller bandwidth of the cavity means that we can use a pulse oscillating closer to the resonant frequency without undesirable high transmission below the threshold. For example, transmission of the low-intensity pulse is almost 3 times smaller than in structure 1(a). As a consequence of smaller pulse detuning, we need a smaller index change to shift the resonant frequency. In our simulations, the relative index change on the threshold is 0.54% in the noninstantaneous model. Unfortunately, the large  $Q$  factor of the defect cavity increases the switching time and magnifies the dispersion in transmitted pulse. This fundamental trade-off is highly problematic for applications to switching in optical telecommunications.

The structure shown in Fig. 1(c) is quite different from those of Figs. 1(a) and 1(b). Unlike the Fabry-Perot geometry of Figs. 1(a) and 1(b), the side-coupled cavity geometry reflects only frequencies near the resonant frequency, while all other frequencies are transmitted. In order to study switching, in this case, we use a pulse with central frequency equal to the resonant frequency of the cavity. In our numerical experiments we assumed noninstantaneous nonlinearity in high-dielectric rods. In the low-intensity regime the transmission is about 17% and this value can be reduced using a more narrow pulse. For example, if we use the pulse with 2 times longer duration time or with FWHM  $\Delta\omega=0.00011(2\pi c/a)$ , transmission in the low-intensity regime is reduced to 6% [Fig. 3(e)]. If we increase the input pulse intensity, the resonant frequency changes and transmission for different frequencies is allowed or prohibited. If the input pulse has very large energy, a small part of this energy can be enough to change the properties of the cavity while the major part of the narrow pulse can pass through the waveguide with negligible interaction with the cavity. Unfortunately, this device does not have a sharp threshold like the Fabry-Perot geometry. Such a sharp change in transmission as a function of intensity may be required for many optical switching applications.

#### IV. SWITCHING OF PULSE TRANSMISSION BY A CONTINUOUS WAVE

In order to study the possible control of optical pulses by the second laser beam, we consider a pulse propagating together with a continuous wave (cw) in structure 1(a). We launch the same pulses as in Sec. III, but now together with a continuous wave oscillating with frequency equal to the resonant frequency of the defect cavity. The cw laser acts as a gate. By changing the intensity of the cw field it is possible to modulate the transmission of the laser pulse. For very intense cw fields, it is also possible to transfer energy from the cw field to the pulse through oscillations in the nonlinear refractive index of the microresonator. However, these effects involve almost prohibitively high field intensities. We use two sets of Maxwell's equations coupled through nonlinear interaction to describe the state of each beam with time. As mentioned earlier, this description is possible when the pulse spectral components are well separated from that of the cw field. Transmission of the pulse strongly depends on the continuous-wave power. For very small continuous-wave

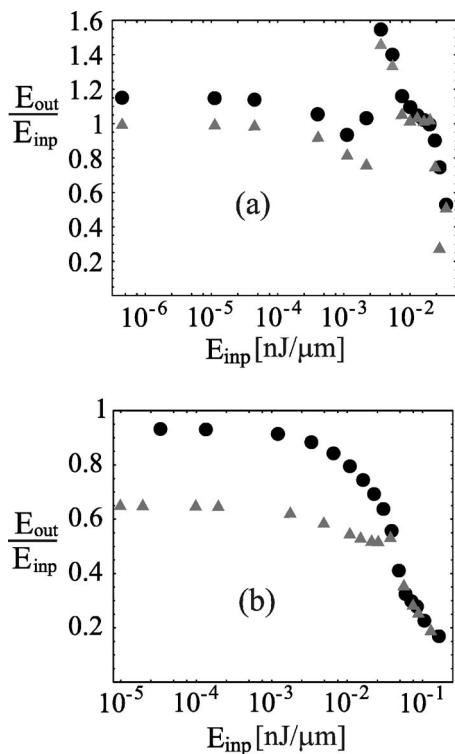


FIG. 7. (a) Transmission energy  $E_{out}$  relative to pulse input energy  $E_{inp}$  as a function of input pulse energy of a Gaussian pulse [with spectral FWHM,  $\Delta\omega=0.00022(2\pi c/a)$ ] propagating through the waveguide shown in Fig. 1(a), together with a continuous wave whose intensity acts as a control parameter. Input powers of continuous waves are (a) for the instantaneous model,  $2.4 \text{ W}/\mu\text{m}$  (black circles) and  $1.8 \text{ W}/\mu\text{m}$  (grey triangles) and (b) for the noninstantaneous model  $18 \text{ W}/\mu\text{m}$  (black circles) and  $12 \text{ W}/\mu\text{m}$  (grey triangles). In all cases the center frequency of the input pulse,  $\omega_0=0.2573(2\pi c/a)$ , is detuned from the Fabry-Perot resonance at  $\omega_{res,1a}=0.2581(2\pi c/a)$  and the cw laser is in resonance with the microcavity.

power, the properties of the defect cavity are determined predominantly by the pulse energies and the continuous wave does not have an influence on the transmitted spectrum. By increasing the continuous-wave power up to a characteristic value of  $2.5 \text{ W}/\mu\text{m}$  in the instantaneous model (or  $18 \text{ W}/\mu\text{m}$  in the noninstantaneous model), transmission is enhanced for all input pulse intensities. However, a further increase of the continuous-wave power has the opposite influence on pulse transmission. At the threshold intensity of the cw field and for low enough input pulse energy, transmission is very high and there is no dispersion in the transmitted spectrum (Figs. 7 and 8). In the instantaneous model we find that transmission can reach 115% in the low-input-pulse-energy regime, while this value is slightly smaller (93%) in the noninstantaneous model. Nonlinear properties of defect cavity depend on the total field whose amplitude oscillates with a period comparable to the cavity buildup time. When the time-dependent oscillations of the nonlinear refractive index [see Fig. 9(a)] contain spectral components at the difference frequency between the pulse and the cw laser field, it is possible to exchange energy between the beams. If we increase the pulse intensity, the energy trans-

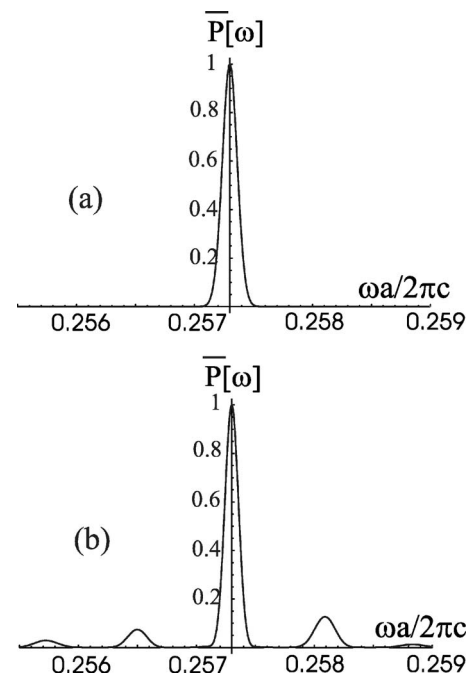


FIG. 8. (a) Output power profile of the Gaussian pulse, with input spectral FWHM  $\Delta\omega=0.00022(2\pi c/a)$ , propagating through the waveguide depicted in Fig. 1(a), in the presence of a continuous wave whose input power is  $18 \text{ W}/\mu\text{m}$ . Input pulse energies are (a)  $0.13 \text{ pJ}/\mu\text{m}$  and (b)  $30 \text{ pJ}/\mu\text{m}$ . Here, we consider only the noninstantaneous model (see text) for nonlinear Kerr response. In both cases, the input pulse center frequency  $\omega_0=0.2573(2\pi c/a)$  is detuned from the Fabry-Perot microcavity resonance at  $\omega_{res,1a}=0.2581(2\pi c/a)$ , whereas the cw field is on resonance.

ferred from the continuous wave takes a smaller and smaller part in the energy of the transmitted pulse and, at the same time, the spectral intensity of the pulse with new frequencies  $\omega_0 \pm (\omega_{res} - \omega_0)$  becomes visible. A further increase of the pulse intensity makes the induced index change of the nonlinear cavity more dependent on the pulse intensity. The index oscillation amplitude increases and the oscillation period changes. This influences the amount of exchanged energy between the beams. At the same time, dispersion in the transmitted spectrum becomes higher and higher and the pulse is more and more distorted.

We calculated, numerically, the switching time for the beam coupling device in the low-pulse-intensity regime, and we found it to be comparable to the linear cavity decay rate. A pulse propagating through the waveguide needs approximately the cavity buildup time in order to cross the cavity. Consequently, a high- $Q$  cavity device slows down the transfer of information through the optical network. The same time scale arises when we switch the pulse from a transmitting state to a reflecting state by turning off the continuous wave. Accordingly, we identify this time scale as the switching time of the device.

We perform similar simulations for a pulse propagating through the waveguide with higher- $Q$ -factor cavity in the noninstantaneous model. In this case, the pulse is detuned by a smaller amount from the linear cavity resonance as described in Sec. III. Qualitatively, these two systems behave in

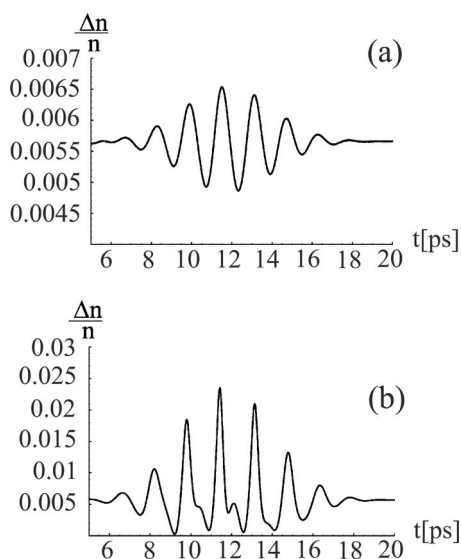


FIG. 9. (a) The time dependence of the refractive index change at one point, in the large defect rod, near its front surface and in the middle of defect line of the structure depicted in Fig. 1(a). The pulse with input energy (a) 0.1 pJ/μm and (b) 37 pJ/μm propagates together with a continuous wave whose input power is 12 W/μm. Here, we consider only the noninstantaneous model (see text) for nonlinear Kerr response. The input pulse amplitude is Gaussian with FWHM  $\Delta\omega=0.00022(2\pi c/a)$  and central frequency  $\omega_0=0.2573(2\pi c/a)$ , while the cw laser field oscillates at the linear resonance of the defect cavity,  $\omega_{cw}=\omega_{res,1a}=0.2581(2\pi c/a)$ .

a similar way. We find maximal transmission of 58% in the low-input-pulse regime. However, the pulse is stretched in time. The time required for the pulse to cross the cavity is not the only parameter which determines the operation time of the device. The cavity buildup time and low group velocity in the cavity provide a lower bound on the temporal duration of a useful pulse. If we want the Gaussian pulse to keep its profile in time, we require a Gaussian pulse with characteristic parameter  $\tau_p$  a few times larger than the cavity decay rate  $\tau_b$ . For example, using a Gaussian pulse with characteristic parameter  $\tau_p=2.5\tau_b\approx 10$  ps, the pulse remains close to Gaussian with  $\tau_p$  enlarged by less than 10% relative to the input pulse profile. Pulses with longer temporal duration have a stronger interaction with the defect cavity and continuous wave. This is apparent in the transmitted energy. Transmission of this pulse, supported by a continuous wave of 4.8W/μm, is 90% in the low-input-pulse-intensity regime. In this case, the relative index change is 0.3%, or equivalently, the maximal electric field in the large dielectric rod is near to 4 MV/cm. This is above the dielectric breakdown field strength for GaAs [26,27]. We conclude that transistor-type “control of light with light” is impractical in this device geometry with Kerr nonlinearity. The switching field strength can be reduced by taking into account specific characteristics of nonlinearity in the engineered vacuum of photonic band-gap materials [5,11,28].

Finally, we study the influence of a continuous wave on pulse propagation through the side-coupled cavity structure of Fig. 1(c) in two different ways. In the first case, we consider a continuous wave oscillating on the cavity resonant

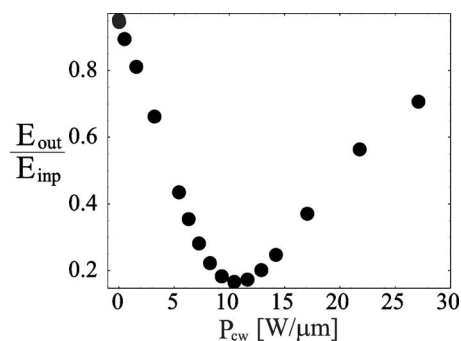


FIG. 10. (a) Transmission energy  $E_{out}$  relative to pulse input energy  $E_{inp}$  of the pulse with very low input energy, propagating through the waveguide shown in Fig. 1(c), together with a continuous wave, as a function of the continuous-wave power measured per 1 μm of the length normal to the 2D microchip plane. The input pulse is Gaussian with FWHM  $\Delta\omega=0.00022(2\pi c/a)$  and central frequency of the pulse is dislocated to  $\omega_0=0.264(2\pi c/a)$ , from the linear resonance  $\omega_{res,1c}=0.2646(2\pi c/a)$ , whereas the continuous wave is on resonance. Here, we consider only the noninstantaneous model (see text) for nonlinear Kerr response.

frequency, passing through the waveguide. Afterwards, we launch a pulse detuned to  $\omega_0=0.264(2\pi c/a)$ . For very low continuous-wave power, almost all pulse energy bypasses the cavity because the pulse oscillates out of resonance with negligible interaction between the pulse and cavity. As we increase the continuous-wave power, the nonlinear shift of the cavity resonant frequency enables the cavity to resonate with the pulse at frequency  $\omega_0$  (see Fig. 10). This device enables light to be switched from pulse transmission to pulse reflection. Unfortunately, this device needs large continuous-wave power (10 W/μm) since the nonlinear effect dislocates the continuous wave from the cavity resonance and only a small part of the continuous wave enters the cavity. In the second case, we exchange frequencies of the continuous wave and the pulse. In this case, the pulse energy is mostly reflected before the nonlinearity takes effect because the pulse oscillates on resonant frequency. For an incident pulse of 5.2 ps duration,<sup>1</sup> we have a transmission of 17% (in the absence of the continuous wave) because of the large bandwidth of the pulse. This ambient transmission can be reduced if we use pulses of longer time duration. The continuous wave oscillates out of resonance, and only a small part of it enters the cavity. When the resonant frequency reaches the frequency of the continuous wave, the cavity will absorb and accumulate the light energy, leading to a significant change of the resonant frequency. As a result, the pulse can pass through the waveguide without reflection [Fig. 11(a)]. There is no interaction of the pulse with the defect cavity, so the transmission on threshold jumps to 97% and the pulse identity is retained [Fig. 11(b)].

## V. CONCLUSIONS

In summary, we have investigated all-optical switching in nonlinear two-dimensional photonic crystal waveguides,

<sup>1</sup>We define the pulse duration as a time for which the amplitude of the pulse remains above 1/2 of its maximum.

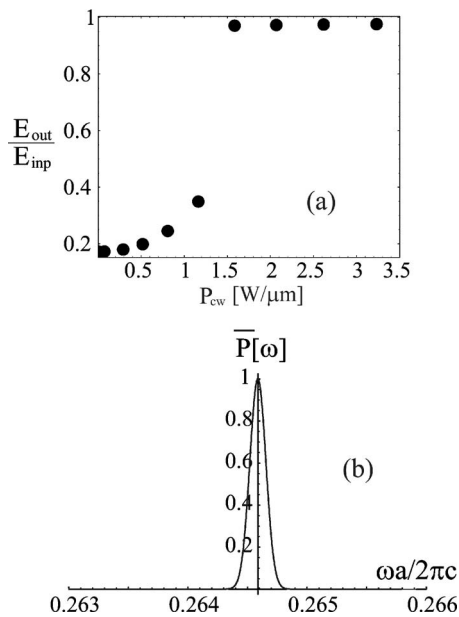


FIG. 11. (a) Transmission energy  $E_{out}$  relative to pulse input energy  $E_{imp}$  of a Gaussian pulse [with spectral FWHM,  $\Delta\omega = 0.00022(2\pi c/a)$ ] with very low input energy, propagating through the waveguide shown in Fig. 1(c), together with a continuous wave, as a function of input cw power in the waveguide channel, measured in units of watts per 1  $\mu\text{m}$  of the length normal to the 2D microchip plane. In this case the center frequency of the input pulse,  $\omega_0 = 0.2646(2\pi c/a)$ , is the same as the linear Fabry-Perot resonance, whereas the cw field is detuned to  $\omega_{cw} = 0.264(2\pi c/a)$ . (b) Transmitted power profile of the pulse on threshold. Here, we consider only the noninstantaneous model (see text) for nonlinear Kerr response.

coupled to resonant defect cavities. For comparison purposes, we considered the PC waveguide structure introduced in Ref. [13]. We analyzed the detailed temporal and spectral features of the switching phenomenon. We compared the specific properties of three different types of defect cavities and two types of Kerr nonlinear response.

Our numerical simulations, made on waveguides containing nonlinear Fabry-Perot resonators, confirm that a laser pulse with high enough intensity can change the resonant frequency of the structure, allowing switching from pulse reflection to transmission. But a more detailed investigation reveals that this device suffers from fundamental limitations and trade-offs for applications in optical telecommunications. For realistic choices of the cavity quality factor, we find an unreasonably large refractive index change in the cavity region near the switching threshold. For the instantaneous model of Kerr nonlinear response, we calculated maximal relative index change of 4.4% on the threshold. For the more physically realistic noninstantaneous model of Kerr nonlinear response, the relative index change (of 0.87%) is about 5 times smaller, but still extremely large. This maximal index change is about 2 times larger than estimated by the simple physical picture provided in the Introduction. This is because the defect rod is not illuminated evenly. Instead, the borders of the defect rod are intensely illuminated, while the center of the dielectric rod is weakly illuminated. We con-

clude that the simplified model described in the Introduction estimates the average index change in the defect rod and provides only a lower bound on the peak value of the index change. Additional reduction of the threshold field intensity and index change can be achieved by smaller detuning of the pulse from the linear resonance. However, in this case we have to use a defect cavity with higher  $Q$  factor, leading to longer switching and pulse duration times. For example, our simulations on the high- $Q$ , Fabry-Perot, resonator structure of Fig. 1(b) gave a maximal relative index change of  $\Delta n/n = 0.5\%$  for the noninstantaneous model and  $\Delta n/n = 3\%$  for the instantaneous model. These are nevertheless extremely high for the typical semiconductors used in optoelectronics. For an ideal switching device, we require a nonlinear shift of the entire cavity bandwidth from the spectral range of the pulse. At the same time we need a short switching time. These two conditions can be satisfied only with the use of materials with extraordinarily large nonlinear response. This is unlikely with nonlinear materials described by the instantaneous Kerr response model. Most significantly, our study shows that the switching mechanism consists not only of a steady-state nonlinear shift of the band structure by the signal beam, but rather it is dominated by an active interaction and feedback between the microcavity and the laser pulse. As a consequence of this interaction, we detect dispersion in the transmitted pulse for all simulations with input pulse intensity above the threshold. In the side-coupled microcavity structure of Fig. 1(c), a high-intensity laser pulse keeps its frequency profile after crossing the cavity, but this type of cavity does not have a sharp threshold as desired in switching devices. For these various reasons, nonlinear self-switching of pulse in photonic crystal waveguides with a Kerr-nonlinear microcavity faces serious challenges for practical deployment in optical telecommunications. A new paradigm may also be required for all-optical transistors to become competitive with their electronic counterparts.

Finally we analyzed switching of a pulse by a secondary continuous wave detuned from the pulse spectrum, but propagating through the same PC waveguide. For light propagation in the nonlinear Fabry-Perot structure of Fig. 1(a), we found that the transmitted energy of the laser pulse can, in some cases, exceed 100%, due to nonlinear exchange of energy from the continuous-wave laser to the pulse. This is a direct consequence of nonlinear “ringing” effects in the cavity refractive index. For low enough input pulse intensity, dispersion in the transmitted pulse can be very small. While this property is advantageous for practical applications, this requires cw laser intensities that are near the threshold for dielectric breakdown in the semiconductor. In the structure of Fig. 1(c), the cavity is physically dislocated from the waveguide. Here, the weak interaction between the pulse and defect cavity (when they are spectrally detuned from each other) implies that the cavity does not distort the transmitted pulse. However, as in the previous structures, the power of the continuous wave and the maximal induced nonlinear index shift is exceedingly high. These results suggest the importance of considering alternative forms of nonlinear response (such as that arising from the embedding of resonant quantum dots within or near the photonic crystal waveguide) [8–11,28] in the quest for practical “control of light with light” in photonic band-gap materials.

- [1] S. John, Phys. Rev. Lett. **58**, 2486 (1987).
- [2] E. Yablonovitch, Phys. Rev. Lett. **58**, 2059 (1987).
- [3] S. John, Phys. Rev. Lett. **53**, 2169 (1984).
- [4] A. Chutinan, S. John, and O. Toader, Phys. Rev. Lett. **90**, 123901 (2003).
- [5] S. John, O. Toader, and K. Busch, *Photonic Band Gap Materials: Semiconductors of Light*, 3rd ed., Vol. 12 of *Encyclopedia of Physical Science and Technology*, edited by Robert A. Meyers (Academic Press, San Diego, 2002), p. 133.
- [6] E. Yablonovitch, Sci. Am. **285** (6), 47 (2001).
- [7] J. D. Joannopoulos, P. R. Villeneuve, and S. Fan, Nature (London) **386**, 143 (1997).
- [8] S. John and T. Quang, Phys. Rev. Lett. **78**, 1888 (1997).
- [9] S. John and M. Florescu, J. Opt. A, Pure Appl. Opt. **3**, S103 (2001).
- [10] M. Florescu and S. John, Phys. Rev. A **69**, 053810 (2004).
- [11] R. Wang and S. John, Phys. Rev. A **70**, 043805 (2004).
- [12] H. M. Gibbs, S. L. McCall, and T. N. C. Venkatesan, Phys. Rev. Lett. **36**, 1135 (1976); H. M. Gibbs, *Optical Bistability: Controlling Light with Light* (Academic Press, New York, 1985).
- [13] M. Soljačić, M. Ibanescu, S. G. Johnson, Y. Fink, and J. D. Joannopoulos, Phys. Rev. E **66**, 055601(R) (2002).
- [14] M. Soljačić, C. Luo, and J. D. Joannopoulos, Opt. Lett. **28**, 673 (2003).
- [15] S. F. Mingaleev and Y. S. Kivshar, J. Opt. Soc. Am. B **19**, 2241 (2002).
- [16] M. F. Yanik, S. Fan, and M. Soljačić, Appl. Phys. Lett. **83**, 2739 (2003).
- [17] M. Florescu and S. John, Phys. Rev. A **64**, 033801 (2001).
- [18] S. G. Johnson, S. Fan, P. R. Villeneuve, J. D. Joannopoulos, and L. A. Kolodziejski, Phys. Rev. B **60**, 5751 (1999).
- [19] S. J. McNab, N. Moll, and Y. A. Vlasov, Opt. Express **11**, 2927 (2003).
- [20] A. Taflove and S. C. Hagness, *Computational Electrodynamics* (Artech House, Norwood, MA, 2000).
- [21] M. Koshiba and Y. Tsuji, IEEE Microw. Wirel. Compon. Lett. **11**, 152 (2001).
- [22] Robert W. Boyd, *Nonlinear Optics*, 2nd ed. (Academic Press, San Diego, 2003).
- [23] K. W. DeLong, C. L. Ladera, R. Trebino, B. Kohler, and K. R. Wilson, Opt. Lett. **20**, 486 (1995).
- [24] G. Stegeman and P. Likamwa, in *Nonlinear Optical Materials and Devices for Applications in Information Technology*, edited by A. Miller, K. R. Welford, and B. Daino (Kluwer Academic, Dordrecht, 1995), p. 285.
- [25] J. D. Joannopoulos *et al.*, United States Patent No. 6,058,127 (2000).
- [26] K. Shenai, R. S. Scott, and B. J. Baliga, IEEE Trans. Electron Devices **36**, 1811 (1989).
- [27] F. Lappenberger, K. F. Renk, R. Sammer, L. Keldysh, B. Rieder, and W. Wegscheider, Appl. Phys. Lett. **83**, 704 (2003), and references therein.
- [28] Sajeev John and Tran Quang, Phys. Rev. Lett. **76**, 2484 (1996).